Journal of Applied Mechanics and Technical Physics, Vol. 38, No. 6, 1997

RADIOGRAPHIC OBSERVATION OF LIQUID FILTRATION THROUGH AN OIL-BEARING ROCK

E. I. Pal'chikov

UDC 621.386+550.8

The goal of the present paper is to elucidate the possibility of developing a simple radiographic procedure for observing the shape and position of liquid boundaries inside a low-porosity compact medium (oil-bearing sandstone) at the impregnation stage. The pore volume amounts to 10–15% of the sample volume. The liquid (water or oil) leads to an insignificant change in density. The similarity between the atomic masses of the water components (O^{16} and H^1) and the oil components (C^{12} and H^1) and between the water and oil stoichiometry [H_2O and $(CH_2)_n$)] complicates the observation of the water–oil interface against the background of a rock layer.

The computer tomography of oil-bearing rock samples performed in [1] is too complex to be used in an ordinary research laboratory. The procedure proposed in [2] has a number of disadvantages: the variation in the radiation spectra with the distance traveled in the material is ignored, special programs are required for image processing, and the measurement accuracy is affected by the nonideal character of the characteristic curve of an x-ray film. Sprunt et al. [1] and Tidwell and Glass [2] studied samples that were already impregnated with a liquid.

Knowledge of the impregnation mechanism of a dry sample with water and oil is essential to the preparation of samples in studies of the dynamics of displacement of oil by water in an oil-bearing rock.

It has been of interest to experimentally obtain answers to the following question.

1. Which forces are determining in the impregnation of a natural sample with a size of ~30 mm — capillary or gravitational?

2. What is the result of the competition between water and oil under mirror-symmetric boundary conditions when impregnation proceeds simultaneously from two opposite ends of the sample? Where will water and oil meet and what shape will the boundary take?

3. What is the rate of the impregnation process and how rapidly are equilibrium conditions established?

4. What is the size of the pores that determine the impregnation rate?

Description of the Experiment. For the experiment we used a purified dried sample of sandstone 30.7 mm long and 29 mm in diameter taken from a well No. 838 of the Mortym'ya-Teterevskoe deposit. A sample with laboratory number 1179–85 was provided by the joint-stock company "LUKOIL–Uraineftegaz." Its parameters were as follows: the sampling range 1586–1592 m, core extent 4.5 m, distance of the place of sampling from the top 3.1 m, open porosity 5.7%, rock density 2.26 g/cm^3, and gas permeability 0.0028 μm^2. Oil and attendant water were taken from the same deposit. Sample 1 was glued by a silicon sealant 4 into a boat 5 made of a thin aluminum foil, as shown in Fig. 1a.

For free exit of air from the rock volume in the initial stage of the experiment, a gap 6 of about 0.2 mm was left between the lateral surface of the sample and the boat wall. Oil 2 and water 3 were poured simultaneously from different sides to a height approximately equal to half the diameter of the sample. The end was wetted only partially to observe the upward motion of the liquid under the action of capillary forces. To improve contrast, we added the x-ray contrast substance KI to distilled water to a concentration of 0.1 mole of solution. It was assumed that this should not change radically the interaction of water with the rock, because,

Lavrent'ev Institute of Hydrodynamics, Siberian Division, Russian Academy of Sciences, Novosibirsk 630090. Translated from Prikladnaya Mekhanika i Tekhnicheskaya Fizika, Vol. 38, No. 6, pp. 169–177, November–December, 1997. Original article submitted March 20, 1996.

0021-8944/97/3806-0963 $18.00

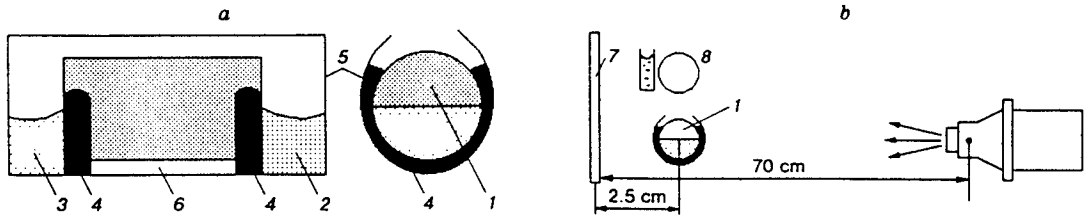

Fig. 1

in reality, solutions of alkali metal halides are present in attendant water. X-ray contrast substances were not added to the oil lest the contrast of the oil–water boundary inside the rock sample decreases.

The radiation source was a pulsed frequency x-ray device fabricated at our laboratory. The maximum voltage across the tube was 150 kV, and the effective energy of radiated quanta was 75 keV. The design and principle of operation of the device are similar to those described in [3].

The focus of the x-ray tube was located at 70 cm from the film, and the center of the sample was located at 2.5 cm from the film. Figure 1b shows a schematic diagram of the experimental arrangement. X-ray photographs were taken on a PMK film 7 without amplifying shields. The exposure was sufficient for the exposure curve to enter a linear portion with $\gamma = 3$–4, for which the photographic width of the x-ray film is best realized. The radiation dose was monitored by a DK-02 dosimeter and was 0.83 R at 70 cm from the focus. The film was treated by the "Rentgen-2" developer for 7 min. To simplify subsequent digital processing, particular attention was given to the constancy of the development time (accuracy of 30 sec) and of the developer temperature (±0.5°C).

Digitization of Images. Negative images were input in transmitted light with a scanner of the firm "Kora," designed on the basis of a line of LF1024-25/1 silicon photodiodes produced by the firm "Vostok" (Novosibirsk). For input of images in transmitted light, we fabricated an illuminator with a uniform exposure field. It consisted of eight rows of luminescent lamps and a focusing diffuser separated by ~10 mm from the sharp negative image plane. By means of a lens, the image was projected on a line of 1024 photodetectors, which was moved in the transverse direction by a stepping engine. The scale and spatial resolution of the input image were controlled by varying the distance from the lens to the negative image and by setting an extension tube.

The blackening range in an x-ray film far exceeds the standard 8-bit range used in IBM-compatible computers for gray half-tone images. During image input by means of the scanner's hardware-software, we compressed the dynamic range by γ-correction with a gamma of $\gamma = -4$ to avoid loss of information available in the x-ray photographs. With allowance for the intrinsic gamma of the PMK film ($\gamma \approx 4$), this transformation simultaneously linearized the transfer function of the image obtained, thus facilitating the subsequent quantitative processing of the brightness signal. As a result of digitization, all x-ray photographs were transferred to tiff-format files, and further work was performed with them.

Processing of Digitized Images. The coordinates and brightness of points in photographs were measured by means of the Aldus PhotoStyler package for Windows. A spatial resolution of 11 pixels per 1 mm allowed measurements of the distance in x-ray photographs with accuracy not worse than ±0.05 mm.

Before quantitative determination of the location and shape of the liquid front in the sample, we performed median averaging with a cell size of 3 × 3 to decrease the grain noise of the film. With allowance for the size of the focus of the x-ray source and the film–sample and the film–focus distances, this practically did not deteriorate the spatial resolution of x-ray photographs.

Because of the obvious inaccuracy of the simple exponential model for the absorption law of polychromatic x-ray radiation, we used a procedure for measuring the thickness of the liquid layer in which a calibrating wedge 8 of the tested materials was taken simultaneously with the sample on the same film [a wedge-like vessel with water imposed along the axis on the dry rock sample (Fig. 1b)]. The walls of the wedge-like vessel were made of the same foil as the boat in which the impregnated sample was glued. For a narrow longitudinal fragment of the wedge image, the histogram of distribution of pixels in brightness

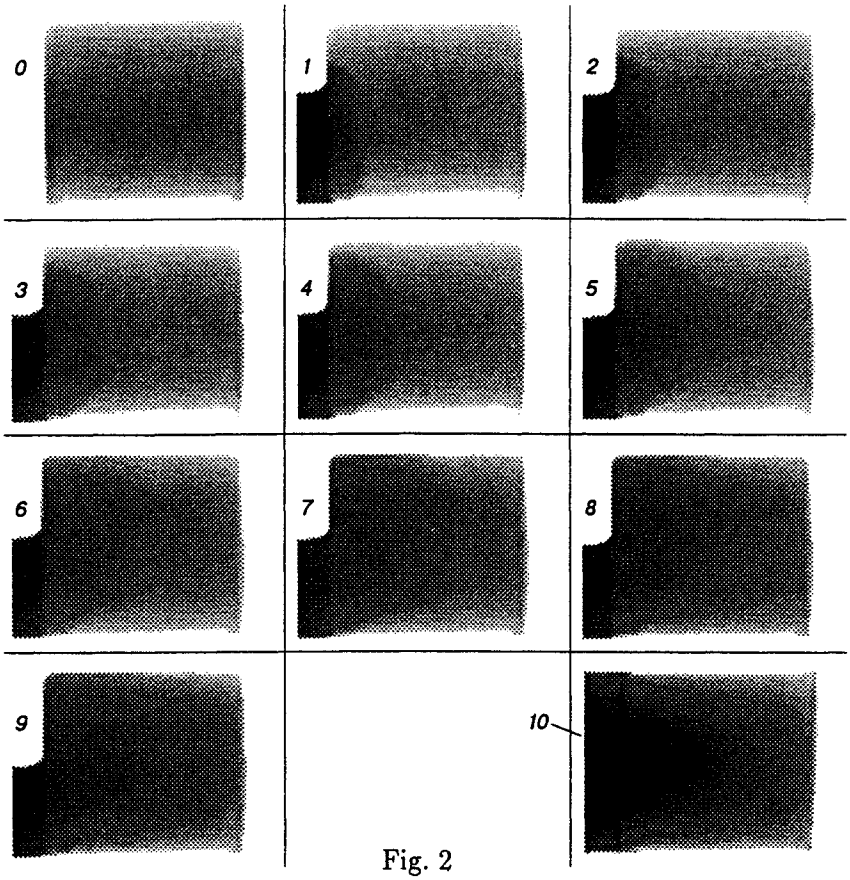

Fig. 2

was transformed to a linear distribution using "Gray Color Map" transforms, γ-corrections, and selection of brightness and contrast. Then, the selected transforms were applied to the entire image. This allowed us to compare the brightness of the image along the axis of the sample and the water concentration using a simple linear calibrating function.

To observe the shape of the liquid front on the monitor screen after linearization and calibration, we used posterization (treatment of a half-tone picture by a step transfer function) with numbers of step from 4 to 16. Using the procedure of finding contours, we obtained a picture of isophots, which was input on paper as a solid copy.

When it was necessary to eliminate from consideration the effect of the density of the material and the shape of the rock sample, in the stage of half-tone processing the original image of the rock sample obtained before impregnation was subtracted from the photograph studied.

In constructing curves of water distribution along the sample versus the coordinate, of the entire tiff file we used data of one line that passed through the center of the sample along its axis.

Discussion of the Results. Figure 2 shows the experimental data as half-tone photograph Nos. 0–10, and Table 1 and Figs. 3–5 shows the data in quantitative form. Photograph No. 0 is a still picture before the beginning of the experiment. In each of the next photographs, water is located to the left of the sample, and oil is located to the right. Photograph Nos. 1–3, taken 3.5, 9.5, and 19.5 min later, show that, within the first 20 min, water most rapidly penetrates deep into the lower part of the sample, traveling $\approx$5 mm in 3.5 min and $\approx$10 mm in 20 min, i.e., about one third of the length of the sample. This advance is most probably associated with the gravitational drop in pressure. After 30 min (photograph No. 4), a ledge appears on the liquid boundary on the lower left at 4.7 mm from the edge of the sample. It is apparently associated with oil, which has rapidly penetrated through the slot between the sample and the boat and impregnated the bottom and sides of the sample. That oil rapidly penetrated into this slot was evident from the sample and also from the rapid decrease in the oil level (flow rate 0.63 ml) in the first 10 min and the slow decrease in the oil level

TABLE 1

Photograph number (Fig. 2)	Time of photography, min	Position of the base of the front	Position of the front at half-height	Front width at half-height	Flow rate of water, ml
		mm			
1	3.5	6.10	4.33	1.77	0.20
2	9.5	8.31	6.54	1.77	0.31
3	19.5	11.32	8.93	2.39	0.45
4	30	13.35	10.52	2.83	0.49
5	60	17.07	12.65	4.42	0.67
6	120	19.19	13.62	5.57	0.91
7	240	22.38	15.92	6.46	0.91
8	720	27.68	19.90	7.78	1.20
9	1510	30.6	22.11	8.49	1.25
10	1520	30.6	22.11	8.49	1.25

Note. Sample length 30.6 mm (346 pixels), diameter 29.0 mm, noise 8 pixels (±0.35 mm).

(flow rate 0.064 ml) in the next 10 min.

After wetting the surface from below and from the sides along the generatrix of the cylindrical sample, oil begins to enter deep into the interior, preventing penetration of water there. The resulting ledge remains unchanged within 24 h, i.e., in all the subsequent photographs. Apparently, because of the occurrence of oil at the bottom and because of the almost complete wetting of the entire left end of the sample with water, which rises under the action of capillary forces, after 30 min the advance of the water front into the interior is already greater at the center of the sample rather than at the bottom (photograph No. 4). The entry of water, due to capillary forces, at the generatrix of the cylinder at the top abruptly changes the boundary conditions for some time. Within 60 min (photograph No. 5), the water front extends farthest into the interior in the upper and middle parts of the sample. Precisely at this time (60 min), the front reaches the middle of the sample (15.6 mm) and would have met with the oil front if it behaved symmetrically. But this is not observed visually. The water front travels further 19.3 mm, now along the center of the sample, in 2 h (photograph No. 6), 24 mm in 4 h, 26.5 mm in 12 h, and, within 12–25 h, it reaches the far end of the sample and becomes more and more indistinct and smeared.

After 2 and 4 h (photograph Nos. 6 and 7, respectively), it can be seen that in the bottom part of the sample the boundary as if breaks up into two fronts, one of which lags behind the other by 5.4 and 6.8 mm, respectively. Photograph No. 10, taken from above, shows that this can be explained by the formation, on the side, of stepped regions occupied by oil.

Thus, as can be seen from half-tone photographs (Fig. 2), oil occupied the edges of the entire sample, and the corners and periphery of its right part, forming a concave bowl, and water extended as a tongue from the left end along the axis of the sample.

In addition, photograph Nos. 8 and 9 show that, at the top left, water traveled 15 mm along the surface of the cylinder to the middle of the sample, due to capillary forces, and did not let oil there. This looks especially strange in the photograph, because visual inspection showed that, at the top left, the outside of the sample is entirely coated with oil, and water in the cell to the left of the sample is coated with an oil film as well.

Quantitative Analysis of the Liquid-Front Propagation. Figure 3 shows the same phases of the process as those in Fig. 2, after 3×3 median filtration, calibration, posterization into 16 steps of brightness, and differentiation of boundaries. The images obtained in the form of isophots safely suggest that, within 12–25 h, water at various concentrations penetrates into all parts of the rock sample. However, the axisymmetric picture of isophots, due to the cylindrical shape of the starting rock sample, strongly distorts the distribution pattern of water density.

Figure 4 shows the water-density distribution ignoring the effects of the shape and material of the rock

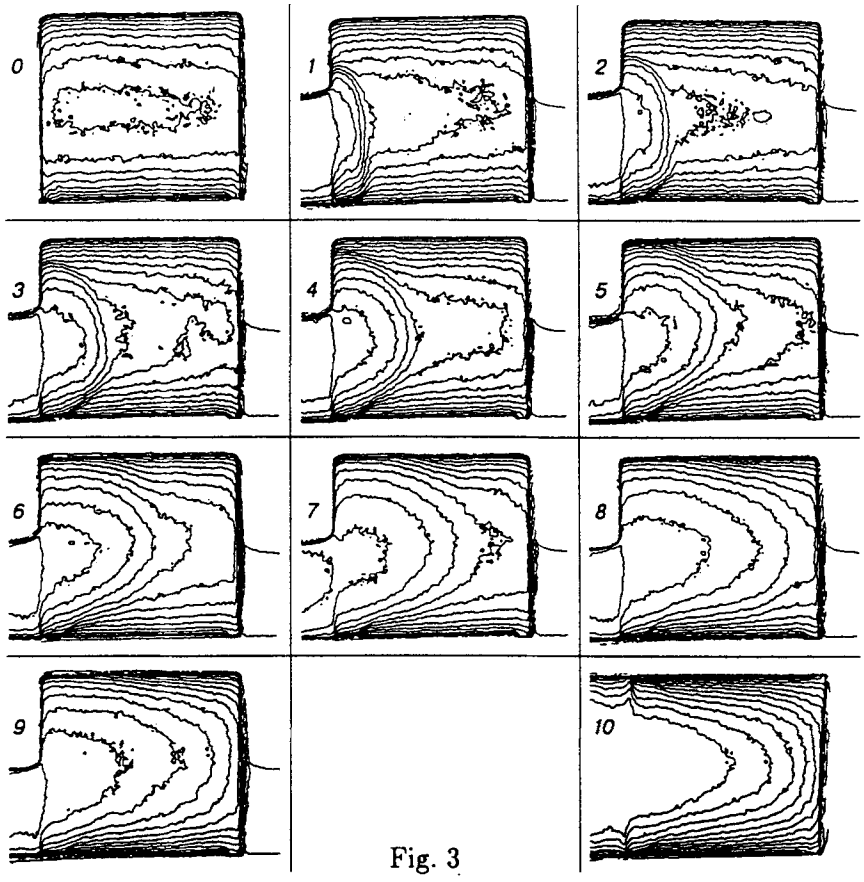

Fig. 3

sample. For this, after median filtration and calibration, image No. 0 of the dry rock sample, taken before the experiment, was subtracted from each image in Fig. 2. Then, we performed linear scale transformation of brightness (because the brightness range became narrower after the subtraction), posterization into eight brightness steps, and differentiation of boundaries. Since subtraction of images deteriorates the signal–noise ratio, the number of gradations during posterization was decreased to eight. Photograph Nos. 1–6 in Fig. 4 (t = 120 min) are consistent with photograph Nos. 1–6 in Figs. 2 and 3, but the water front in the first three photographs becomes flatter, and the boundary at the ledge on the lower left becomes more distinct.

The difference from the previous images begins with photograph No. 7 in Fig. 4 (t = 240 min), which shows that water begins to markedly interact with oil. The presence of oil does not permit water to propagate along the center of the right part of the sample as rapidly as in the upper right part of the sample. In the left upper part, an insignificant amount of oil that penetrated affected the shape of the water-density distribution by forcing the isophot lines back. In photograph No. 9 in Fig. 4 (t = 1510 min), the isophots have reversed curvature and the region occupied predominantly by oil is shown. The mirror-symmetric S-shaped structure of isophots formed in later stages shows that, in the lower left corner of the sample there is more water present, and in the right lower corner there is more oil present. In the upper part of the sample, the concentration gradient along the sample is smaller by one band than in the lower part. Thus, the contribution of the gravitation mechanism to the steady concentration distribution amounts to $\sim 1/7$ of the capillary mechanism. It is interesting to note that, in the top view (photograph No. 1 in Fig. 4), all S-shaped distortions of the isophots are absent, because averaging along the vertical results in sufficiently flat shapes of the water front with approach to the right end of the sample.

The quantitative analysis of the liquid propagation along the axial line of the sample using digital processing of photograph Nos. 1–9 in Fig. 2 is shown in Fig. 5 (curves 1–9, respectively), where the sample density is plotted on the vertical and the coordinate is plotted on the horizontal. For convenience of comparison, the curves are constructed with a shift along the conditional third axis. The range from 60 to 90 rel. units

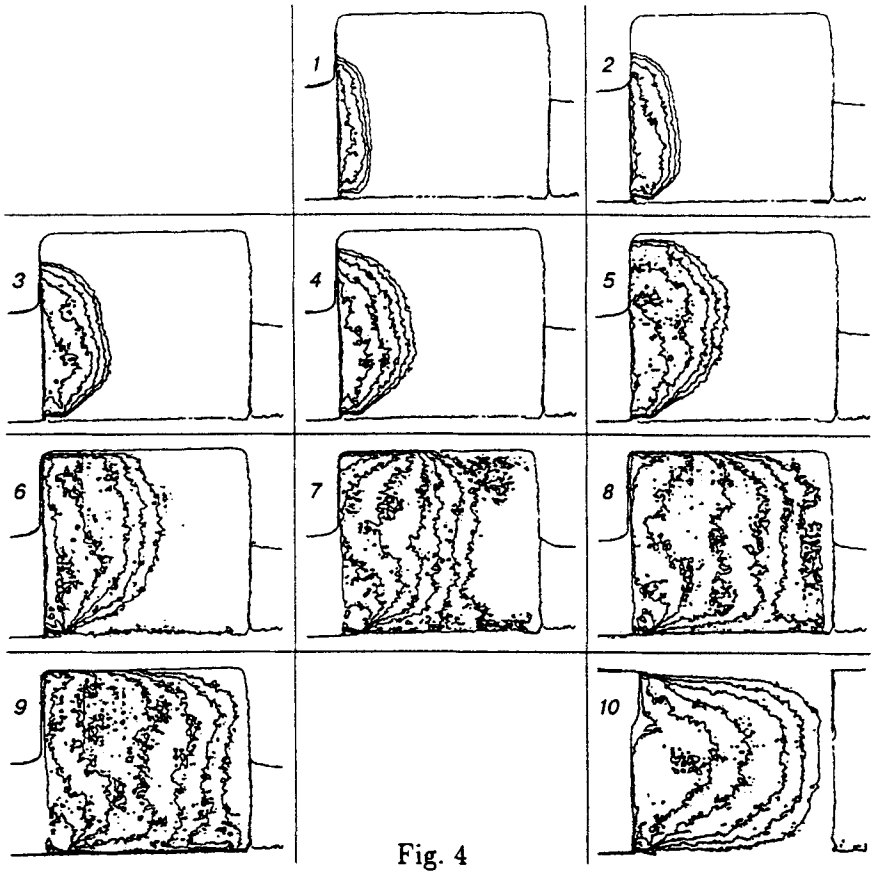

Fig. 4

corresponds, with accuracy not worse than ±1.5 units, to the range of water volume concentrations from 0 to 15% (or the range of pore saturation from 0 to 100%).

Table 1 gives the results of measurements of the water-front parameters.

Analysis of Figs. 4 and 5 and also the smooth smearing of the water boundary in the photographs in Figs. 2–4 and in the curves in Fig. 5 indicates that we are dealing with a complex branched network of capillaries filled with water, oil, and gas. In the early stages (at $t \leqslant 60$ min), the filling of voids is mainly affected by the interaction of media at the ternary interface: water–air–capillary walls (or oil–air–capillary walls). In the later stages (at $t \geqslant 60$ min), the final distribution of concentrations in the sample before the onset of equilibrium is governed by the interaction of media at the quaternary boundary: water–oil–air–capillary walls. Measuring the liquid level in a cuvette in the x-ray photographs, it is possible to estimate the water flow rate (see Table 1) and its final concentration in the sample. For example, within 25 h, 1249 mm^3 of water entered the sample, which amounts to 7.1% of the total volume of the sample. Taking into account that the porosity of the sample is ~15%, we can state that, despite the complex shape of the interface, oil and water occupy roughly equal amounts of voids in the sample.

If we assume as a first approximation that a pore of the sample is a capillary of circular cross section with length L and radius R, the flow rate Q is described by the Poiseuille flow $Q = \pi \Delta P R^4/(8\eta L)$, where ΔP is the difference in pressure and η is the liquid viscosity.

For slow filling of a horizontal capillary from one end ignoring the flow of the variable mass, the relation $Q\,dt = \pi R^2\,dL$ is valid. Hence it follows that the propagation of the liquid front under the action of the difference in pressure is described by the relation $L = R\sqrt{\Delta P t/(4\eta)}$.

If the difference in pressure is caused only by surface-tension forces, the condition $\Delta P = 2\sigma/R$ leads to the following dependence of the distance traveled by the front on time and the radius of the capillary:

$$L = \sqrt{\sigma R t/(2\eta)}. \tag{1}$$

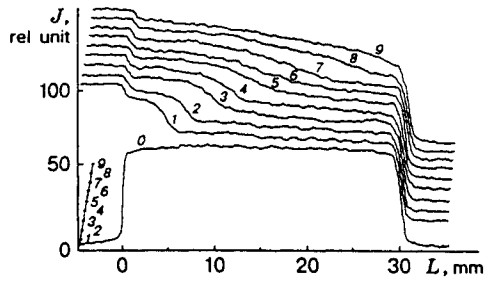

Fig. 5

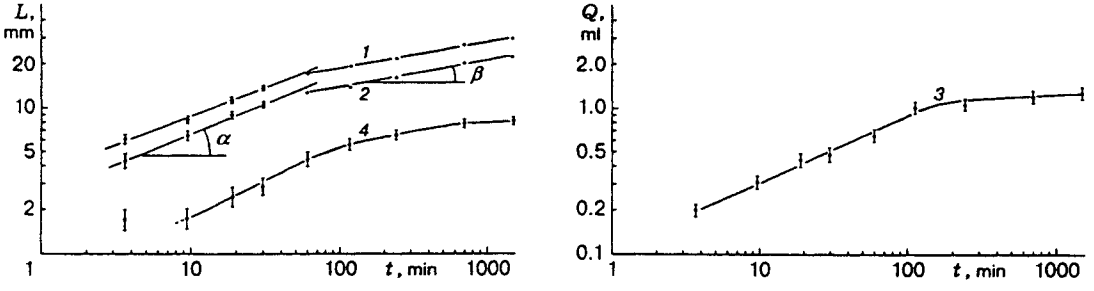

Fig. 6

From the results in Table 1, one can construct plots of the position of the water front in the sample (Fig. 6) in a double logarithmic scale. The benchmarks of experimental errors in Fig. 6 show the standard deviations for samples of experimental data obtained by a series of close parallel tracings of digital images. The absence of a benchmark indicates that the error is smaller than the size of the point in Fig. 6. Curves 1 and 2 show the positions of the front measured at half-height and at the base. The slope of the curves $\tan\alpha = 0.4$–0.5 indicates that, for the first 60 min, the filling is adequately described by a model with an exponent of 1/2 according to relation (1) for a circular capillary. Then, the slope decreases to $\tan\beta = 1/6$, which apparently corresponds to the propagation of water through capillaries which are already partially occupied by oil. A certain decrease in the slope $\tan\alpha$ with respect to 0.5 in the dry sample can be explained by the fact that the set-up of the experiment was not quite one-dimensional: at later times, the boundary of the water front is not flat, and the interfacial area increases. Curve 3 (liquid flow rate) agrees well with curves 1 and 2.

The characteristic cross-sectional area of a capillary, which is responsible for water propagation, is estimated as

$$R = \frac{2\eta L^2}{\sigma t} = \frac{2 \cdot 10^{-2}\,[\mathrm{g/(cm \cdot sec)}] \cdot 1\,[\mathrm{cm^2}]}{73\,[\mathrm{dyn/cm}] \cdot 1320\,[\mathrm{sec}]} \sim 3 \cdot 10^{-7}\,[\mathrm{cm}].$$

From this it follows that only part of the liquid that fills the capillaries is entrained in flow, because the microphotographs show that the sample contains larger capillaries through which according (1) the liquid should propagate more rapidly. The smooth front of increase in density in x-ray photographs indicates that only part of the capillaries in this region is occupied by the liquid. On the one hand, the nonuniform structure of the capillaries and the presence of small branches retard the propagation of the liquid front in the main large capillary. On the other hand, at any wetting angle smaller than 90°, they ensure forward propagation of the ternary interface and a state similar to complete wetting of the walls of large capillaries. Thus, large capillaries are filled after the filling of smaller lateral branches, and precisely this process determines the propagation of most of the water in the sample. Flows of such type are described in [4, 5] and are not unusual.

The experiment shows that the half-width of the liquid front measured from the base to the half-height (curve 4 in Fig. 6) changes with time roughly by the same law as the coordinate of the position of the front itself. The half-width of the front in this case is always about 1/4 of the distance traveled by the front. At

t = 3.5 min, the first point drops out of consideration, because the exposure time is comparable with the time of front propagation to its half-height. The slope for the most characteristic time interval of 10–60 min, when the impregnation of the sample with water proceeds without marked influence of oil, is 0.5 with good accuracy. This suggests that the proposed capillary model is also applicable for the process of smearing of the front.

Conclusions. The tests performed show that pulsed radiography with the proposed digital processing of images allows one:

- to determine the position and shape of the liquid front inside an oil-bearing sandstone and also the percent content of the liquid in various parts of the sample,
- to trace the dynamics of liquid distribution in the sample,
- to refine models that describe the behavior of liquids in oil-bearing rocks using the dynamics of x-ray photographs.

It is shown in the present work that, during impregnation of a dry sample with a size of about 3 cm at all times, the position of the liquid front inside the volume and on the surface of the sample is determined primarily by capillary effects. The correction due to gravity forces is 10–20%. A significant part of the pore space is not used in the propagation of the liquid front. It is most probable that the liquid does not enter these pores or stays near the walls. The characteristic time of impregnation of the sample from two sides by oil and water before the interaction of the fronts is about 60 min. The state of equilibrium is attained within about 24 h. After the attainment of equilibrium, a gradual decrease in the average concentration of each of the components from 100% to 0 along the entire sample is observed. With allowance for the shape of pores of the sample and the immiscibility of the components, the equilibrium interface between oil and water is a complex volume structure, which is reminiscent of two joined roots, and, in principle, can be of a fractal character.

The experimental radiographic procedures developed in this work can be used for measurements and accurate diagnostics of fluid flows in models of an oil collector.

The author is grateful to S. V. Sukhinin, A. S. Besov, and S. P. Taratuta for their assistance and useful discussions of the results of this work.

REFERENCES

1. E. S. Sprunt, K. P. Desal, M. E. Coles, et al., "CT-scan-monitored electrical-resistivity measurements show problems achieving homogeneous saturation," *SPE Formation Evaluation*, **6**, No. 3, 134–140 (1991).
2. V. C. Tidwell and R. J. Glass, "X-ray visible light transmission for laboratory measurement of two-dimensional saturation fields in thin-slab systems," *Water Resour. Res.*, **30**, No. 11, 2873–2882 (1994).
3. A. A. Altukhov, E. I. Bichenkov, E. A. Gusev, et al., "High-current pulsed x-ray device for dynamic radiography," in: *Prib. Tekh. Éksp.*, No. 1, 189–192 (1986).
4. A. É. Sheider, *Physics of Fluid Flows through Porous Media* [in Russian], Gostoptekhizdat, Moscow (1960).
5. A. G. Ar'e, *Physical Foundations of Filtration of Underground Water* [in Russian], Nedra, Moscow (1984).